



Dihydropyridine Fluorophores Allow for Specific Detection of Human Antibodies in Serum

Domljanovic, Ivana; Rexen Ulven, Elisabeth; Ulven, Trond; Thomsen, Rasmus P.; Okholm, Anders H.; Kjems, Jørgen; Voss, Anne; Taskova, Maria; Astakhova, Kira

Published in:
ACS Omega

Link to article, DOI:
[10.1021/acsomega.8b00424](https://doi.org/10.1021/acsomega.8b00424)

Publication date:
2018

Document Version
Publisher's PDF, also known as Version of record

[Link back to DTU Orbit](#)

Citation (APA):
Domljanovic, I., Rexen Ulven, E., Ulven, T., Thomsen, R. P., Okholm, A. H., Kjems, J., Voss, A., Taskova, M., & Astakhova, K. (2018). Dihydropyridine Fluorophores Allow for Specific Detection of Human Antibodies in Serum. *ACS Omega*, 3(7), 7580-7586. <https://doi.org/10.1021/acsomega.8b00424>

General rights

Copyright and moral rights for the publications made accessible in the public portal are retained by the authors and/or other copyright owners and it is a condition of accessing publications that users recognise and abide by the legal requirements associated with these rights.

- Users may download and print one copy of any publication from the public portal for the purpose of private study or research.
- You may not further distribute the material or use it for any profit-making activity or commercial gain
- You may freely distribute the URL identifying the publication in the public portal

If you believe that this document breaches copyright please contact us providing details, and we will remove access to the work immediately and investigate your claim.

Dihydropyridine Fluorophores Allow for Specific Detection of Human Antibodies in Serum

Ivana Domljanovic,^{†,‡,▽} Elisabeth Rexen Ulven,^{‡,▽} Trond Ulven,^{§,¶} Rasmus P. Thomsen,^{||} Anders H. Okholm,^{||} Jørgen Kjems,^{||,⊥} Anne Voss,[#] Maria Taskova,[†] and Kira Astakhova^{*,†,¶}

[†]Department of Chemistry, Technical University of Denmark, Kemitorvet 206, 2800 Kongens Lyngby, Denmark

[‡]Department of Physics, Chemistry and Pharmacy, University of Southern Denmark, Campusvej 55, 5230 Odense M, Denmark

[§]Department of Drug Design and Pharmacology, University of Copenhagen, Universitetsparken 2, 2100 Copenhagen, Denmark

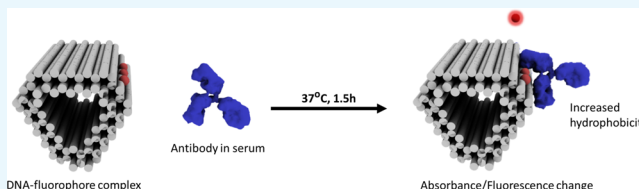
^{||}Interdisciplinary Nanoscience Center (iNANO), Aarhus University, Gustav Wieds Vej 14, 8000 Aarhus C, Denmark

[⊥]Department of Molecular Biology and Genetics, Aarhus University, C.F. Møllers Allé 3, 8000 Aarhus C, Denmark

[#]Department of Rheumatology, Odense University Hospital, J. B. Winsløvs Vej 19, 2, 5000 Odense C, Denmark

Supporting Information

ABSTRACT: Antigen recognition by antibodies plays an important role in human biology and in the development of diseases. This interaction provides a basis for multiple diagnostic assays and is a guide for treatments. We have developed dihydropyridine-based fluorophores that form stable complexes with double-stranded DNA and upon recognition of the antibodies to DNA (anti-DNA) provide an optical response. The fluorophores described herein have advantageous optical properties compared to those of the currently available dyes making them valuable for research and clinical diagnostics. By studying a series of novel fluorophores, crucial parameters for the design were established, providing the required sensitivity and specificity in the detection of antibodies. Using these DNA–fluorophore complexes in a direct immunofluorescence assay, antibodies to DNA are specifically detected in 80 patients diagnosed with an autoimmune disease, systemic lupus erythematosus. Positivity indicated by emission change of α -(4'-O-methoxyphenyl)-2-furyl dihydropyridine strongly correlates with other disease biomarkers and autoimmune arthritis.



1. INTRODUCTION

Antibodies are proteins of key importance that provide defense against cancer, bacteria, and viruses.¹ However, in autoimmune diseases, antibodies attack one's own cells and tissues.² To prevent the disease development, autoimmune antibodies have to be diagnosed early and a treatment has to be started.

Among others, antibodies to nuclear components of cells (antinuclear antibodies) and to double-stranded DNA (dsDNA) are distinctive biomarkers of systemic lupus erythematosus (SLE), a chronic autoimmune disease with multiple manifestations, and life-threatening damage to human organism.^{3,4} Recent studies point at the broad range of autoimmune conditions that involve highly reactive anti-double-stranded DNA (a-dsDNA) antibodies as well.⁵

Detection of antibodies is currently performed either by indirect immunoassays or by direct detection methods.⁶ The indirect methods are usually carried out by variants of the enzyme-linked immunosorbent assay (ELISA) and are widely used.⁷ Direct detection can be done by fluorescence microscopy, surface plasmon resonance, or fluorometry.^{8–10} ELISA is highly sensitive but time demanding and rather costly. The direct methods are simpler in handling, more accurate in target quantification, and inexpensive compared with ELISA.^{8–10}

The key to successful detection of any antibody is a properly designed and highly pure antigen.¹⁰ Synthetic oligonucleotides represent an emerging class of antigens for the detection and study of autoimmune antibodies. We and others recently proved the utility of rationally designed dsDNA molecules in the diagnostics of SLE.^{10–12} Using these antigens and the commercially available dye Eva green, we were able to detect the antibody–DNA interaction by a simple fluorometry assay (Figure 1).¹⁰ Several studies addressed the issue of the DNA sequence recognition by the antibodies.^{10–14} Nevertheless, new dyes with improved properties for the direct immunofluorescence are on demand. In particular, high optical sensitivity to DNA and antibodies would be advantageous to increase specificity of the assay.

DNA origami is an exciting research and diagnostic tool that allows for sensitive detection of a broad range of targets.¹⁵ Origami can be folded into the various shapes, ranging from a nanobox to flat sheet, by adding a set of synthetic oligonucleotide primers to the large viral DNA strand.¹⁵ Reaching a size of 100 nm, DNA origami has a plethora of

Received: March 6, 2018

Accepted: June 26, 2018

Published: July 10, 2018

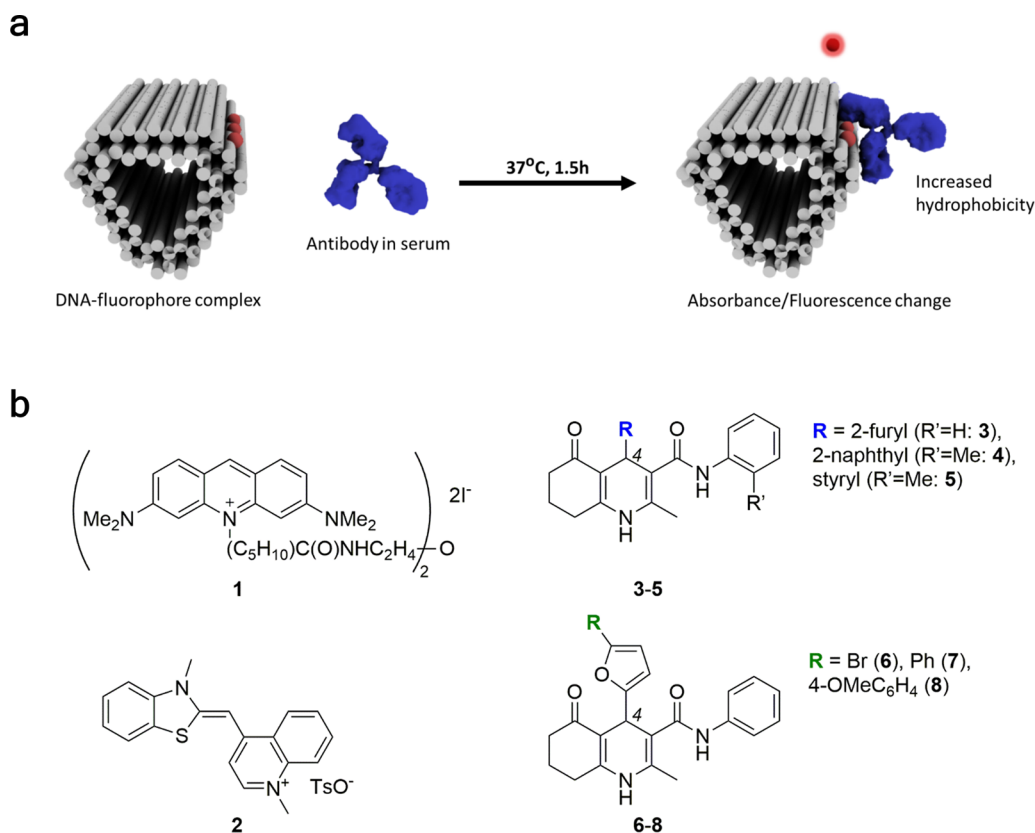
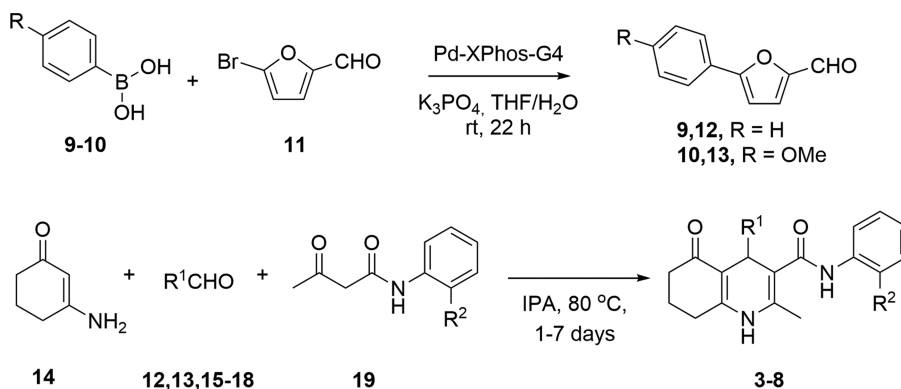


Figure 1. (a) General principle of the immunofluorescence assay; (b) commercially available DNA binding dyes and novel fluorophores used in this work. Eva green (1), thiazole orange (2), and novel dihydropyridines (DHPs 3–8).

Scheme 1. Synthesis of Dihydropyridines 3–8^a



^a $R^1 = 2\text{-furyl } (3, 15), 2\text{-naphthyl } (4, 16), \text{styryl } (5, 17), \alpha\text{-Br-2-furyl } (6, 18), \alpha\text{-Ph-2-furyl } (7, 12), \text{ and } \alpha\text{-(4'-O-methoxyphenyl)-2-furyl } (8, 13).$ $R^2 = \text{H or Me. IPA = isopropyl alcohol.}$

binding sites for fluorophores, small drugs, and biomolecules, being hence an excellent tool to enhance the recognition and detection efficacy per sample volume.¹⁵ Specifically, a complex of DNA origami with noncovalent DNA binding dye can be used as an antigen for the detection of anti-DNA antibodies in biofluids (Figure 1a). Upon the antibody binding, a fluorophore molecules get released from the DNA origami, providing a simple fluorescence read out for the assay.¹⁶

We aimed at developing novel fluorophores with advantageous properties in the direct detection of human antibodies. To address this, we designed, synthesized, and tested novel derivatives of dihydropyridine (DHP; Figure 1b). DHP is a parent of a class of molecules that effectively recognizes

proteins.¹⁷ In particular, DHPs are well known in pharmacology as L-type calcium channel blockers, used in the treatment of hypertension. Our rationale for choosing the DHP scaffold is that the fine tuning of the substitution pattern allows for the optimization of the DNA/protein recognition and of its optical properties. DHP analogues were additionally decorated with planar aromatic moieties and hydrophilic substituents that can provide stacking interactions and hydrogen bonds with large DNA origami.^{10,16} In this article, we describe the design and synthesis of these new fluorophores and prove their ability to specifically detect human antibodies to DNA in blood samples.

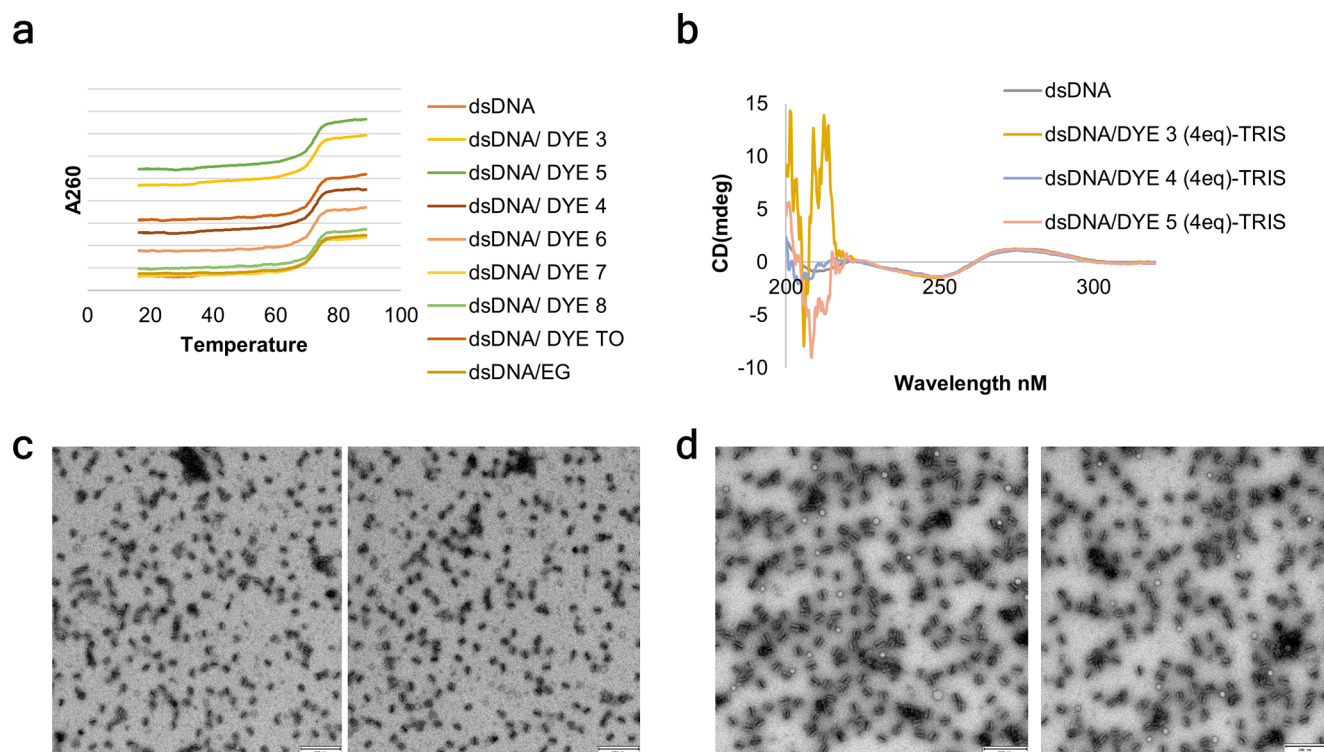


Figure 2. Characterization of DNA duplexes and origami upon adding the fluorophores. (a) T_m study; (b) CD; (c, d) transmission electron microscopy (TEM). (a, b) Experiments were carried out in 100 mM Tris–HCl buffer, pH 7.5, using 0.5 μ M (T_m) or 2 μ M (CD) DNA samples. Double-stranded DNA sequence: (5′-TGT GGT AGT TGA GCG GAT GGC GTA GGC A-3′): (5′-TGC CTA CGC CAT CCG CTC AAC TAC CAC A-3′). (c, d) TEM characterization of prism A incubated with no dye (c), and with 250 mM dye 8 added during annealing. For every sample, two chosen representative TEM images are shown with a scale bar of 200 nm. This image gallery confirms the stability of the prism A in the presence of the dye.

2. RESULTS AND DISCUSSION

Optical sensitivity of organic molecules to their microenvironment is a fundament of multiple tests. However, several biological phenomena require a fine tuning of the sensor's optical properties. A particularly challenging task is to develop a fluorophore that allows for a sensitive and specific detection by interaction with antigen and antibodies. Commercially available fluorophores are developed to effectively recognize either DNA or proteins, but none allow us to monitor the switch in recognition of these two biomolecules.

In this study, our goal was to develop a fluorescent molecule that would allow us to form a bright complex with well-defined DNA origami structures able to bind and detect anti-dsDNA antibodies. To address this, we started with a scaffold that is well known to bind to proteins, dihydropyridine (DHP). By chemical functionalization we achieved the required sensitivity and specificity of a DHP–furan derivative and proved its efficacy in a direct immunofluorescence assay.

For the fluorophore design, we used available knowledge on DNA binding by organic molecules, which combine π – π interactions and hydrogen bonding.^{15,16} Furthermore, extending the aromatic system is known to increase the fluorescent quantum yield and redshift the emission wavelengths.¹⁸ Therefore, we functionalized position 4 of the DHPs (shown in Figure 1) with several aromatic residues, potentially influencing optical properties and biorecognition. For compound 3, we introduced additional aromatic substituents at the furan, resulting in compounds 6, 7, and 8 (Figure 1). Methyl groups were removed in several fluorophores to study the effect on DNA and antibody recognition.

Owing to their medical significance, the synthesis of DHP derivatives has been widely explored.^{19,20} A straightforward scaffold diversification was developed for the rapid preparation of all of the designed fluorophores. The synthesis of the fluorophores is shown in Scheme 1. In brief, boronic acids **9** were reacted with furfurals **11** resulting in derivatives **12–13**. Incubation of products **12–13**, along with commercially available aldehydes **15–18**, with 3-aminocyclohex-2-en-1-one (**14**) and 3-oxo-*N*-arylbutanamides (**19**) provided the DHPs **3–8** in up to 87% yields (see the details on synthesis and characterization in Supporting Information, Chapter 2).

Novel fluorophores were evaluated in three steps. First, optical properties and biorecognition of each fluorophore were investigated. Second, the fluorophores with optimal performance were screened against a panel of dsDNA probes to obtain the brightest complex. Third, the selected fluorophore–DNA complexes were tested in a direct immunofluorescence assay of a-dsDNA in human samples.

Individual fluorophores were analyzed by UV–vis spectroscopy and fluorometry. As expected, the substitution pattern had a strong effect on the optical properties of the fluorophores, for example, fluorescence maximum for compounds **3** vs **8** shifted from 430 to 470 nm in 100 mM phosphate-buffered saline (PBS), pH 7.2 (Supporting Information, Chapter 2). Quantum yields also varied dramatically, with highest values for the fluorophore complexes **4**, **5**, and **8** (0.17–0.40). The molar extinction was similar for all of the dyes and somewhat lower than for previously used thiazole orange, **2** (Supporting Information, Table S1).

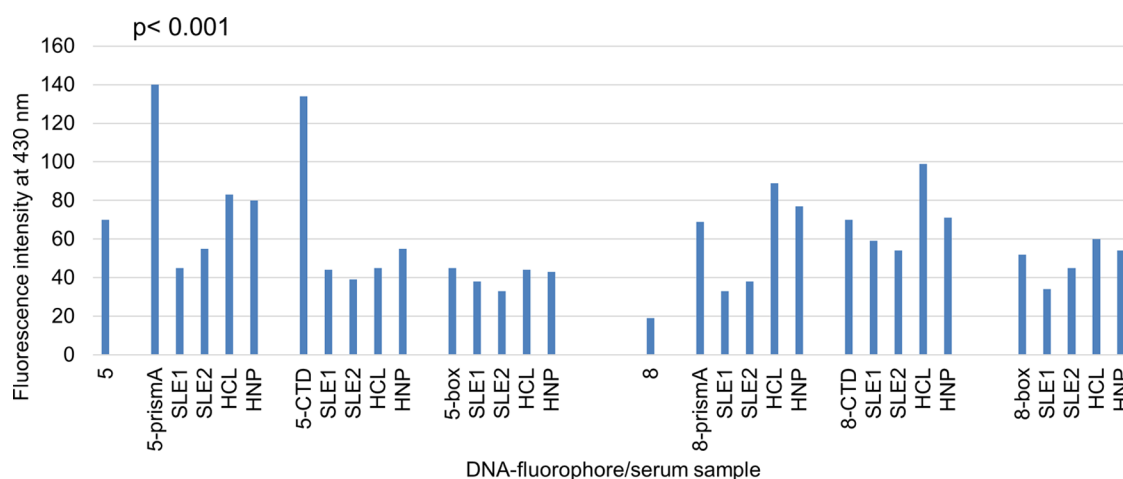


Figure 3. Immunofluorescence screening of DNA origami vs fluorophores 5 and 8. Fluorescence intensities of SLE sera and controls (human anticardiolipin plasma, HCL, and human normal plasma, HNP), upon incubation with 5, 8, and their complexes with DNA origami prism A, calf thymus DNA (CTD), and DNA origami box. The assay was carried out in 100 mM phosphate buffer (pH 7.2) containing 2% BSA, using excitation/emission wavelengths of 360/440 nm (5) or 380/470 nm (8). Each measurement has been done in duplicates. *P* value is given for the one-way analysis of variance (ANOVA) tests of all groups.

In general, all of the fluorophores showed increased fluorescence in the presence of calf thymus DNA (CTD) (Supporting Information, Figure S1). However, compounds 3–4, without DNA, showed no response to the addition of bovine serum albumin (BSA). Remarkably, compound 3 nicely discriminated the DNA (CTD) over a protein (BSA; Supporting Information, Table S1). Fluorescence intensity of compound 3 was slightly increased with CTD and quenched by 2-fold upon addition of 1 mM BSA (Supporting Information, Figure S1). Among all dyes, compound 4 and 8 gave highest brightness (FB) with CTD.

Although compound 3 showed good discrimination of antibodies in SLE-positive sera vs controls, it had a relatively weak fluorescence compared to that of compounds 7 and 8 bound to DNA (Supporting Information, Table S1). Moreover, its absorbance maximum was below 380 nm, which is not suitable for screening by a conventional plate reader.

To gain more information on the fluorophore–DNA complexes, we applied a model dsDNA, a 30-mer fragment of the human genome. Using short dsDNA allowed us to perform thermal denaturation (T_m) and circular dichroism (CD) studies (Figure 2a,b). These well-established methods reveal the stability of the DNA duplex and its structure in the presence of different concentrations of the fluorophores.^{21,22} Eva green and thiazole orange were used as controls. It was surprising that the dyes had a relatively small effect on the thermal stability of model dsDNA (change in $T_m \pm 1.5$ °C, with a measurement precision of ± 0.5 °C). Similarly to Eva green and thiazole orange, CD studies indicated that DHP derivatives 3–5 had little effect on the secondary structure of dsDNA (Supporting Information, Chapter 3). A possible interaction mode of fluorophores with DNA could be an intercalation.¹⁸ However, the observed lack of fluorescence quenching and unchanged CD and T_m profiles for compounds 3–5 vs DNA exclude the potential intercalation.¹⁸

To study the effect of the dyes on the stability of large DNA origami, we applied agarose gel electrophoresis and transmission electron microscopy (TEM) (Supporting Information, Figures S5,S6 and 2c,d). For these studies, we selected two representative dyes, 3 and 8, and prism A. Agarose gel of prism A incubated with no dye, 3, or 8 in increasing concentrations

of 50, 250, and 500 mM, revealed a faster migration of the front band. This is evident of proper folding of the prism A in all cases (Supporting Information, Figure S6A). TEM images also confirm a well-defined structure for prism A when dyes 3 and 8 are added (see Supporting Information Figure S6E for 3–prism A TEM).

We aimed at finding the optimal DNA antigen to form a bright and stable complex with fluorophores 5 and 8. We chose 5 and 8 due to their high brightness and affinity toward dsDNA (see Supporting Information, Tables S1 and S2). Recent studies show that large well-defined three-dimensional (3D) DNA origami structures are advantageous in terms of brightness in the direct immunofluorescence assay.^{10,16,23} Following this lead, we screened five previously reported origami structures: box, platform, ring, and two prism variants (Figure 1b).^{10,24–26} Annealing of origami was done as previously described,¹⁰ and the dye of interest was added during the thermal ramp at 65 °C (see Supporting Information Chapter 4 for details). The resulting complexes were studied by fluorimetry in PBS buffer (Supporting Information, Figure S6B) and upon addition of human sera containing antibodies to DNA (Figure 3; SLE1–2). In the absence of sera, prism A and CTD formed bright complexes with 5, whereas 8 had the brightest signal when bound to platform and prism A. The discrimination of binding by fluorescence was highest for 8, reaching 4.7-fold change of intensity, compared with 2.1-fold change showed by 5 (Supporting Information, Figure S6B).

We carried out the direct immunofluorescence detection using 1 nM prism A, with an excess of fluorophore (5 or 8 at 250 nM) and 2 μ L human plasma in 10 μ L incubation buffer (1 g BSA, 200 μ L Tween-20 in 1 L 1× PBS). The samples were incubated at 37 °C for 1.5 h and then analyzed by fluorimetry, as shown in Figure 1a. Antibodies to phospholipid cardiolipin often cross-react with dsDNA.²⁷ Therefore, we included anticardiolipin positive serum as a control along with healthy patient samples (HCL and HNP, respectively). As can be seen in Figure 3, both fluorophores showed increased fluorescence in the presence of origami and CTD. Fluorescence of the complex formed by compound 8 and prism A decreased significantly when adding SLE1 or SLE2 compared to that of the control sera (Supporting Information,

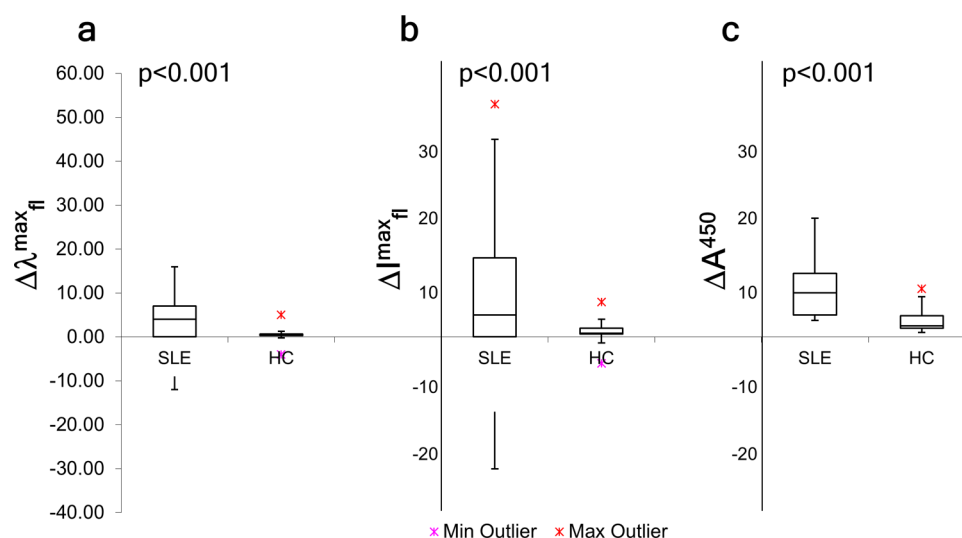


Figure 4. Box-and-whisker plots for the immunofluorescence assay and ELISA. (a) Change in absorbance maximum upon incubation of the complex 8–prism A with patient sera; (b) Change in fluorescence intensity at maximum upon incubation of the complex 8–prism A with sera; (c) Change in absorbance values determined by ELISA as a response to incubation with sera. The data is presented for SLE and healthy controls (HC; number of patients: 80 (SLE) and 60 (HC)). The arms on each boxplot are values $Q_1 - 1.5 \times \text{interquartile range (IQR)}$ and $Q_3 + 1.5 \times \text{IQR}$. Data points for each measurement are mean values for two independent measurements with deviation of the results <3%.

Figure S7). However, using CTD as the DNA scaffold led to a positive response in HCl. Complexes of compound 5 with all origami structures were generally less sensitive to adding SLE sera than those of compound 8 (Figure 3).

To evaluate the role of the 3D dsDNA structure on the fluorophore and a-dsDNA recognition, we repeated the experiments for the origami staple strands in the absence of the scaffold strand, resulting in no dsDNA origami formation (Supporting Information, Chapter 4). In this case, the fluorescence intensity by the dyes was approximately threefold lower than that for the assembled DNA origami structure. Dyes 5 and 8 were also tested without DNA, in which case the sera had no effect on their fluorescence properties (Supporting Information, Figure S7B).

We studied binding kinetics and stoichiometry of prism A with fluorophores 5 and 8 by fluorescence (Supporting Information, Figures S8,S9 and Table S4).²⁸ According to fluorescence titration studies, K_D values for 5 and 8 vs prism A were 2 and 1.1 μM , respectively, which is in the similar range as that for previously reported DNA binding dye Eva green.²⁹ For antibody binding, K_D values for 5 and 8 were approx. 50-fold lower than that for prism A, 40 and 26 nM, respectively (Supporting Information, Table S4).

When the complexes of 5 and 8 with prism A were subjected to interaction with monoclonal anti-dsDNA antibody,¹⁰ K_D values were also within the expected low nanomolar range, 1.25 and 0.24 nM for 5–prism A and 8–prism A, respectively (Supporting Information, Table S4).³⁰ For the negative control (monoclonal antibody to β_2 -microglobulin¹⁰), no binding was observed confirming the specificity of the DNA antigens toward anti-dsDNA antibody (Supporting Information, Figure S10).

Binding stoichiometry was studied by binding isotherms following the described protocol.²⁸ For 5 and 8, the binding ratio of prism A was estimated as 300 mole equivalent of a fluorophore, $\pm 3\%$. In all of the experiments, the results were consistent upon varying the host concentrations.²⁸

The goal of our final study was to explore the properties of compound 8–DNA prism A as a diagnostic tool for antibody

detection in SLE. Compound 8 and prism A have been selected on the basis of the high sensitivity to adding SLE sera and superior quantum yield vs that of 5 (Supporting Information, Table S1). We used a cohort obtained from Odense University Hospital, Denmark, containing 80 adult SLE and 60 healthy control (HC) samples. We benchmarked the performance of compound 8–prism A to a commercial ELISA assay. For this study, the patient samples were selected on the basis of the diagnosed SLE and positivity to antinuclear antibodies determined by a clinical lab. The median age of the SLE-positive patients was 44.7 years and 84% were females. For the experiments, patient sera were diluted 1:100 with standard ELISA diluent. To achieve the required sensitivity and specificity, the molar ratio 8/prism A was optimized for the assay and kept at 250:1 (Supporting Information, Figure S11A). Incubation with dye/dye–prism complex was carried out at 37 °C for 1.5 h. Samples were analyzed by fluorimetry using excitation of 370 nm (8) or 480 nm (Eva green).

We analyzed the position of fluorescence maximum and their intensities for compound 8–DNA prism complex in the presence of human sera (Figure 4; Supporting Information, Tables S6–S9). The mean wavelength for fluorescence maximum was 422 nm, which is 8 nm shorter compared to the emission of the complex of compound 8–prism A in the absence of serum. Minimum and maximum values for the emission shift upon incubation were 0 and –12 nm, respectively.

As for the intensity at emission maximum, 250 nM of compound 8 in SLE sera had intensity of 18 ± 2 arb. units (Supporting Information, Figure S7A). Upon adding 1 nM prism A solution, the intensity increased to 69 ± 2 arb. units. As in the preliminary assay, we observed quenching of fluorescence upon incubation of the compound 8–prism A complex with SLE sera; mean intensity for these samples were reduced to 43 ± 21 arb. units with a rather big deviation among individual samples (Supporting Information, Table S8). We observed a minimum intensity of 17 (quenching) and up to 100 for some samples. Testing healthy controls (HC) gave a cut-off value for the positivity by this assay, which was the

fluorescence intensity change -8 units. In total, 32 SLE samples were found to be positive by both wavelength shift and quenching of fluorescence intensity. However, only 32% positive samples overlapped when the two types of positivity were compared with each other. We carried out sandwich ELISA for SLE samples ($n = 80$), as a control for the assay. In this case, 46% were positive; only 45% of the positives overlapped for the immunofluorescence assay and ELISA.

Having tested healthy controls ($n = 60$), we observed a somewhat similar performance of the fluorescence assay using the prism A/8 complex and the commercial ELISA kit (Figure 4, data for HC cohort). The total number of false positives by ELISA was 6 (10%) vs 4 (7%) for our immunofluorescence assay.

To better understand the predictor role of the a-dsDNA detected by compound 8–prism A, we performed correlation analyses of the obtained antibody levels with clinical features of the patients. The analysis was done for the immunofluorescence and ELISA. Double positivity by emission intensity and wavelength ($n = 32$) did correlate much stronger with arthritis than the result provided by ELISA for these samples (one-way ANOVA test; $p = 3.3 \times 10^{-5}$ compared to 0.68, respectively; Supporting Information Table S11 and Figure S12). We also observed a correlation of a-dsDNA levels determined by the novel immunofluorescence assay with positivity to anti- β 2-glycoprotein I antibodies ($p = 0.014$).

Our result can be further rationalized in terms of polyclonal features of the antibodies. It is common that only 40–70% of the SLE-positive subjects develop high level of a-dsDNA.^{3,6} Therefore, our results of ELISA lie within the expected range of positivity (46%). It is also well documented that ELISA reveals the broad range of antibodies. In turn, the compound 8–prism A complex in the fluorescence assay might be more specific to the antibodies with high affinity.¹⁰ Effective removal of the dye molecules from the antigen, leading to an optical effect, requires high affinity of the antibody to dsDNA which is confirmed by the low dissociation constant of prism A–antibody complex in the presence of 8 (K_D 0.24 nM). This is also in agreement with the stronger correlation of the a-dsDNA determined by compound 8–prism A with clinical features vs ELISA. It is also worth mentioning that ELISA for a-dsDNA is of IgG type only, whereas immunofluorescence also detects other antibody types (IgM, IgA). This could affect the results and correlations with clinical features as well. Lastly, it is remarkable how the substitution in the organic fluorophores allows for the fine tuning of its performance in sensing an antibody. This makes us believe that merging organic synthesis with emerging diagnostic needs could be a new paradigm for assay development, which could positively affect the research and clinical management of difficult conditions such as SLE.

3. CONCLUSIONS

In conclusion, in this study, we prepared and studied new fluorophores for the detection of human antibodies in serum. In the homogeneous immunofluorescence assay, novel DNA–fluorophore complexes show the required features of specificity and sensitivity. This allowed us to screen 80 patient samples diagnosed with an autoimmune disease, SLE, and to define new clinical correlations for the determined antibody levels.

Further development of simple and reliable diagnostic methods for human antibodies have a potential to open up for new possibilities for using organic fluorophores as effective diagnostic tools. In particular, we believe that this simple time-

and cost-effective immunofluorescence approach has much to offer to the rapidly developing field of antibody analysis in biofluids.

4. EXPERIMENTAL SECTION

4.1. General. Synthesis and characterization of fluorophores 3–8 are described in Supporting Information.

All nucleic acid compounds were obtained from Integrated DNA technologies, Inc., Iowa. Fluorescence dyes were purchased from Sigma (TO) and Biotium (EG) and used as received. Calf thymus DNA (CTD) was purchased from Sigma (cat no. D1501).

4.2. Origami Sequences. These were designed and prepared following published procedures.^{10,24–26} Annealing procedures for origami and controls were carried out using 10 nM samples in 1× Tris-acetate-ethylenediaminetetraacetic acid buffer with 12 mM MgCl₂ as follows: lid 100 °C, 90 °C, 2 min, 90 → 60 decrease 0.5 °C per 1 min, 60 → 50 decrease 0.2 °C per 10 min, 50 → 35 decrease 0.5 °C per 1 min; stored at room temperature or 10 °C.

4.3. ELISA Assays. These were made manually following the protocol described recently. Plates were analyzed using a TECAN microplate reader and measuring absorbance at 450 nm. 96-well Maxisorb NUNC microplates were purchased from Thermofisher Scientific.

4.4. Monoclonal Antibody Controls. HYB 290-03 Anti- β 2-Microglobulin (human) clone 12B2 and HYB 331-01 anti-double-stranded DNA clone 3519 available from BioPorto Diagnostics (Hellerup, Denmark) were generously provided by Statens Serum Institute, Copenhagen.¹⁰

4.5. Patient Sera Samples and Healthy Controls. These were obtained from Odense University Hospital, Denmark. Control sera SLE1, SLE2, HCl, and HNP were purchased from a commercial supplier (Immunovision).

4.6. General Protocol for Immunofluorescence Assay. In a microplate, DNA–fluorophore antigen (4 μ L, 10 nM DNA, and 2.5 μ M 8) was mixed with 4 μ L freshly prepared diluent (1 g BSA, 200 μ L Tween-20 in 1 L 1× PBS). Afterward, a 2 μ L predilute serum sample was added (dilution 1:100 with 1 g BSA, 200 μ L Tween-20 in 1 L 1× PBS). Incubation was performed for 1.5 h at 37 °C, followed by immediate fluorescence detection at LightCycler 480 reader (emission at 530 nm).

4.7. Data Analysis. Data analysis was performed in R using one-way ANOVA.³¹

■ ASSOCIATED CONTENT

Supporting Information

The Supporting Information is available free of charge on the ACS Publications website at DOI: 10.1021/acsomega.8b00424.

Experimental details, additional fluorescence, T_m and CD results and graphs, agarose gel electrophoresis pictures, TEM images, demographical and clinical data and statistical analyses (PDF)

■ AUTHOR INFORMATION

Corresponding Author

*E-mail: kiraas@kemi.dtu.dk.

ORCID

Elisabeth Rexen Ulven: 0000-0003-1243-7587

Trond Ulven: 0000-0002-8135-1755

Maria Taskova: 0000-0002-9727-2496

Kira Astakhova: 0000-0003-4878-0301

Author Contributions

[†]I.D. and E.R.U. contributed equally to this work.

Author Contributions

The manuscript was written through contributions of all authors. All authors have given approval to the final version of the manuscript.

Funding

E.R.U. is funded by the Lundbeck Foundation (R181-2014-3247). I.D., M.T., and K.A. are funded by Villum Foundation Young Investigator Programme (13152).

Notes

The authors declare no competing financial interest.

ACKNOWLEDGMENTS

Dr. Alexander Rauch and Prof. Dr. Susanne Mandrup, University of Southern Denmark, are acknowledged for the experimental support of this study.

REFERENCES

- (1) Rider, P.; Carmi, Y.; Cohen, I. Biologics for Targeting Inflammatory Cytokines, Clinical Uses, and Limitations. *Int. J. Cell Biol.* **2016**, *2016*, 1–11.
- (2) Zuily, S.; Domingues, V.; Suty-Seltone, C.; Eschwègef, V.; Bertoletti, L.; Chaouath, A.; Chaouath, F.; Regnault, V.; Horn, M. E.; Erkank, D.; Wah, D. Antiphospholipid antibodies can identify lupus patients at risk of pulmonary hypertension: A systematic review and meta-analysis. *Autoimmun. Rev.* **2017**, *16*, 576–586.
- (3) Pisetsky, D. S. Anti-DNA antibodies — quintessential biomarkers of SLE. *Nat. Rev. Rheumatol.* **2016**, *12*, 102–110.
- (4) Linnik, M. D.; Hu, J. Z.; Heilbrunn, K. R.; Strand, V.; Hurley, F. L.; Joh, T. LJP 394 Investigator Consortium. Relationship between anti-double-stranded DNA antibodies and exacerbation of renal disease in patients with systemic lupus erythematosus. *Arthritis Rheumatol.* **2005**, *52*, 1129–1137.
- (5) Egner, W. The use of laboratory tests in the diagnosis of SLE. *J. Clin. Pathol.* **2000**, *53*, 424–432.
- (6) Pavlovic, M.; Kats, A.; Cavallo, M.; Chen, R.; Hartmann, J. X.; Shoenfeld, Y. Pathogenic and Epiphenomenal Anti-DNA Antibodies in SLE. *Autoimmune Dis.* **2010**, *2010*, 1–18.
- (7) Pillai, S.; Abbas, A. K.; Lichtman, A. H. *Cellular and Molecular Immunology*, 4th ed.; W.B. Saunders Co.: Philadelphia, 2014; Chapter 4, pp 51–87.
- (8) Reich, A.; Marcinow, K.; Bialynicki-Birula, R. The lupus band test in systemic lupus erythematosus patients. *Ther. Clin. Risk Manage.* **2011**, *7*, 27–32.
- (9) Jørgensen, A. S.; Gupta, P.; Wengel, J.; Astakhova, I. K. “Clickable” LNA/DNA probes for fluorescence sensing of nucleic acids and autoimmune antibodies. *Chem. Commun.* **2013**, *49*, 10751–10753.
- (10) Samuelsen, S. V.; Solov'yov, A. I.; Balboni, M. I.; Mellins, E.; Nielsen, T. C.; Heegaard, N. H. H.; Astakhova, K. Synthetic oligonucleotide antigens modified with locked nucleic acids detect disease specific antibodies. *Sci. Rep.* **2016**, *6*, No. 35827.
- (11) Uccellini, M. B.; Busto, P.; Debatis, M.; Marshak-Rothstein, A.; Viglianti, G. A. Selective binding of anti-DNA antibodies to native dsDNA fragments of differing sequence. *Immunol. Lett.* **2012**, *143*, 85–91.
- (12) Buhl, A.; Page, S.; Heegaard, N. H.; von Landenberg, P.; Lippa, P. B. Optical biosensor-based characterization of anti-double-stranded DNA monoclonal antibodies as possible new standards for laboratory tests. *Biosens. Bioelectron.* **2009**, *25*, 198–203.
- (13) Zhu, H.; Lou, H.; Yan, M.; Zou, X.; Li, Q. Z. Autoantigen Microarray for High-throughput Autoantibody Profiling in Systemic Lupus Erythematosus. *Genomics, Proteomics Bioinf.* **2015**, *13*, 210–218.
- (14) Sanguineti, S.; Crowley Centeno, M. J.; Merlo Lodeiro, F. M.; Cerutti, L. M.; Wilson, A. I.; Goldbaum, A. F.; Stanfield, L. R.; de Prat-Gay, G. Specific recognition of a DNA immunogen by its elicited antibody. *J. Mol. Biol.* **2007**, *370*, 183–195.
- (15) Tørring, T.; Voigt, N. V.; Nangreave, J.; Yan, H.; Gothelf, K. V. DNA origami: a quantum leap for self-assembly of complex structures. *Chem. Soc. Rev.* **2011**, *40*, 5636–5646.
- (16) Domljanovic, I.; Carstens, A.; Okholm, A.; Kjems, J.; Nielsen, T. C.; Heegaard, N. H. H.; Astakhova, K. Complexes of DNA with Fluorescent Dyes Are Effective Reagents for Detection of Auto-immune Antibodies. *Sci. Rep.* **2017**, *7*, No. 1925.
- (17) Hudson, B. D.; Christiansen, E.; Murdoch, H.; Jenkins, L.; Hansen, H. A.; Madsen, O.; Ulven, T.; Milligan, G. Complex Pharmacology of Novel Allosteric Free Fatty Acid 3 Receptor Ligands. *Mol. Pharmacol.* **2014**, *86*, 200–206.
- (18) Glazer, A. N.; Rye, H. S. Stable dye-DNA intercalation complexes as reagents for high-sensitivity fluorescence detection. *Nature* **1992**, *359*, 859–861.
- (19) Sharma, V. K.; Singh, S. K. Synthesis, utility and medicinal importance of 1,2- & 1,4-dihydropyridines. *RSC Adv.* **2017**, *7*, 2682–2732.
- (20) Bull, J. A.; Mousseau, J. J.; Pelletier, G.; Charette, A. B. Synthesis of Pyridine and Dihydropyridine Derivatives by Regio- and Stereoselective Addition to N-Activated Pyridines. *Chem. Rev.* **2012**, *112*, 2642–2713.
- (21) Kyrp, J.; Kejnovská, I.; Renciuik, D.; Voricková, M. Circular dichroism and conformational polymorphism of DNA. *Nucleic Acids Res.* **2009**, *37*, 1713–1725.
- (22) Wang, C.; Bae, J. H.; Zhang, D. Y. Native characterization of nucleic acid motif thermodynamics via non-covalent catalysis. *Nat. Commun.* **2015**, *7*, No. 10319.
- (23) Adel, A.; Berkvens, D.; Abatih, E.; Soukheh, A.; Bianchini, J.; Saegerman, C. Evaluation of Immunofluorescence Antibody Test Used for the Diagnosis of *Canine leishmaniasis* in the Mediterranean Basin: A Systematic Review and Meta-Analysis. *PLoS One* **2016**, *11*, No. e0161051.
- (24) Yang, Y.; Zhao, Z.; Zhang, F.; Nangreave, J.; Liu, Y.; Yan, H. Self-Assembly of DNA Rings from Scaffold-Free DNA Tiles. *Nano Lett.* **2013**, *13*, 1862–1866.
- (25) Zancacchi, F. C.; Manzo, C.; Alvarez, A. S.; Derr, N. D.; Garcia-Parajo, M. F.; Lakadamyali, M. A DNA origami platform for quantifying protein copy number in super-resolution. *Nat. Methods.* **2017**, *14*, 789–792.
- (26) Endo, M.; Hidaka, K.; Kato, T.; Namba, K.; Sugiyama, H. DNA Prism Structures Constructed by Folding of Multiple Rectangular Arms. *J. Am. Chem. Soc.* **2009**, *131*, 15570–15571.
- (27) Claypool, S. M.; Koehler, C. M. The Complexity of Cardiolipin in Health and Disease. *Trends Biochem. Sci.* **2012**, *37*, 32–41.
- (28) Thordarson, P. Determining association constants from titration experiments in supramolecular chemistry. *Chem. Soc. Rev.* **2011**, *40*, 1305–1323.
- (29) Mao, F.; Leung, W. Y.; Xin, X. Characterization of Eva Green and the implication of its physicochemical properties for qPCR applications. *BMC Biotechnol.* **2007**, *7*, No. 76.
- (30) Sun, Y. S.; Landry, J. P.; Fei, Y. Y.; Zhu, X. D.; Luo, J. T.; Wang, X. B.; Lam, K. S. Effect of fluorescently labeling protein probes on kinetics of protein-ligand reactions. *Langmuir* **2008**, *24*, 13399–13405.
- (31) R Core Team. *A Language and Environment for Statistical Computing*; R Foundation for Statistical Computing: Vienna, Austria, 2013.